Geophysical Research Letters

RESEARCH LETTER
10.1029/2019GL082226

Ion Behaviors in the Reconnection Diffusion Region of a Corrugated Magnetotail Current Sheet

Shan Wang[1,2], Li-Jen Chen[2], Naoki Bessho[1,2], Michael Hesse[3,4], Barbara L. Giles[2], and Thomas E. Moore[2]

[1]Astronomy Department, University of Maryland, College Park, MD, USA, [2]NASA Goddard Space Flight Center, Greenbelt, MD, USA, [3]Department of Physics and Technology, University of Bergen, Bergen, Norway, [4]Southwest Research Institute San Antonio, San Antonio, TX, USA

Key Points:
- In a flapping magnetotail current sheet, meandering ions accelerated by the out-of-plane electric field are observed
- Lobe ions are accelerated toward the current sheet by the electric field mainly along the local normal
- The current sheet corrugation enhances mixing of demagnetized ions

Correspondence to:
S. Wang,
swang90@umd.edu

Citation:
Wang, S., Chen, L.-J., Bessho, N., Hesse, M., Giles, B. L., & Moore, T. E. (2019). Ion behaviors in the reconnection diffusion region of a corrugated magnetotail current sheet. *Geophysical Research Letters*, *46*, 5014–5020. https://doi.org/10.1029/2019GL082226

Received 26 JAN 2019
Accepted 15 APR 2019
Accepted article online 18 APR 2019
Published online 21 MAY 2019

Abstract The current sheet structure and ion behaviors in a magnetotail reconnection diffusion region are investigated. The multispacecraft analysis suggests a corrugated current sheet structure, interpreted as due to a flapping motion that propagates along geocentric solar magnetospheric along the $+y$ direction in the Geocentric Solar Magnetospheric (GSM) coordinate. The electric field (E) and ion distributions have similarities with those in a planar current sheet. Energetic ions move along the current direction, suggesting the acceleration by the observed reconnection E during the meandering motion. Counterstreaming ions along the current sheet normal suggest the acceleration by the Hall E that is observed to be the dominant component. However, at certain locations, E and counterstreaming ions significantly deviate from the local normal direction, and more than one pair of counterstreaming populations exist, possibly because the corrugated current sheet enables ions entering the current sheet at different locations with different velocities to mix together.

1. Introduction

During magnetic reconnection, ions are significantly energized and take the majority of the dissipated magnetic energy (e.g., Yamada et al., 2014). In the reconnection diffusion region, two important mechanisms contribute to the ion energization. The reconnection electric field is along the reconnection current direction, which is typically the positive y direction in the geocentric solar magnetospheric (GSM) coordinate for magnetotail reconnection. The reconnection electric field accelerates ions during their meandering motion to form an energetic tail at positive V_y in velocity distribution functions (VDFs; e.g., Zenitani et al., 2013). The in-plane (in the GSM x-z plane) electric potential is set up due to the decoupling of ion and electron motion in the diffusion region, with E_z pointing toward the midplane and E_x pointing away from the X-line (e.g., Aunai et al., 2011). Ions are accelerated toward the potential well and forms counterstreaming populations along V_z in VDFs (e.g., Aunai et al., 2011; Nagai et al., 2015; Wygant et al., 2005).

The magnetotail current sheet often has flapping motion, moving up and down (along z) across the steady spacecraft (e.g., Runov et al., 2009; Sergeev et al., 2013, 2004; Zhang et al., 2002). The flapping can be caused by instabilities in the current sheet, for example, kink mode (Karimabadi, Daughton, et al., 2003; Karimabadi, Pritchett, et al., 2003), and is also associated with the solar wind and global magnetosphere conditions (e.g., Sergeev et al., 2008). In addition to the up-and-down motion, the flapping propagates along y with a typical speed of tens of kilometers per second to ~200 km/s (Sergeev et al., 2004).

The understanding of ion dynamics in the reconnection diffusion region has been mostly based on an approximation of a two-dimensional (2D) planar current sheet structure, invariant along the y direction. With the high-resolution measurements of the Magnetospheric Multiscale (MMS) mission (Burch et al., 2015), ion VDF evolution in a flapping current sheet can be resolved, as will be analyzed in this study. The observation suggests that the ion behavior in the reconnection diffusion region mainly resembles that in 2D current sheets as introduced above, while the flapping motion and the associated variations of the current sheet orientation enhance ion mixing leading to effective heating.

2. Data

For the MMS data presented in this study, the ion measurements are from the burst data of the Fast Plasmas Investigation, with a time resolution of 0.15 s (Pollock et al., 2016). Because ion measurements at the

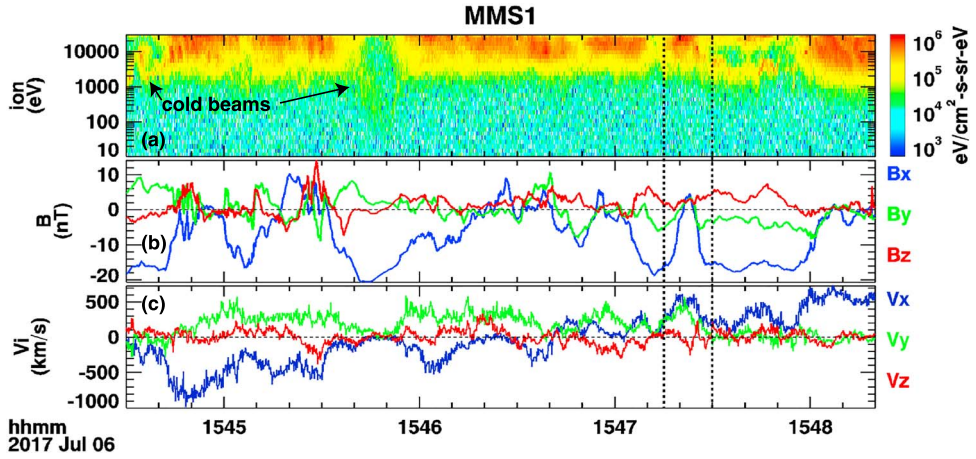

Figure 1. Overview of the magnetotail current sheet observed by MMS1: (a) ion spectrogram; (b) magnetic field in GSM; and (c) ion bulk velocity in GSM. V_{ix} reverses the sign, suggesting a reconnection diffusion region crossing. The interval between the vertical dashed lines is further analyzed as shown in Figure 2. MMS = Magnetospheric Multiscale; GSM = geocentric solar magnetospheric.

magnetotail are contaminated by a random background, we subtract a uniform background from the distribution data. The background is estimated using the average counts below 100 eV (with negligible real data) over 15:46–15:48 UT on 6 July 2017. To improve the counting statistics, the ion distributions are accumulated over four measurements (0.6 s), while all the presented features can also be seen from single-frame distributions. The magnetic field data are from the burst measurements of the fluxgate magnetometer with 128 samples/s (Russell et al., 2016). Electric field data are from the burst measurements of the spin-plane (Lindqvist et al., 2016) and axial (Ergun et al., 2016) double probes with 8,192 samples/s.

3. Observations

MMS crossed the magnetotail at GSM [−24.2, 1.3, 4.5] R_E on 6 July 2017 around 15:45 UT (Figure 1). In the shown interval, the spacecraft transitioned between the lobe and the plasma sheet. The lobe region has cold ion beams (Figure 1a) and strong magnetic fields (Figure 1b), for example, at 15:44:30–15:44:40 UT, 15:45:45–15:45:50 UT. The plasma sheet has hot ions and weak magnetic fields, for example, at 15:46–15:47 UT. In the meantime, the ion bulk velocity has a reversal in V_{ix} (Figure 1c), suggesting the crossing of a reconnection diffusion region.

We further analyze the zoomed-in interval between the dashed lines in Figure 1. Close to the midplane where $B_x = 0$, the x component of the ion bulk velocity perpendicular to the magnetic field is ~500 km/s, much smaller than the x component of the $\boldsymbol{E} \times \boldsymbol{B}$ drift of ~2,000 km/s (not shown). As will be shown in Figure 3, the ion distributions are highly structured during this interval. These features suggest that the location is within the ion diffusion region, where ions are demagnetized. We use the spatiotemporal difference (STD) method to estimate the current sheet orientation and motion (Shi et al., 2005, 2006). The method utilizes the magnetic field differences between the measurements from the four spacecraft, along with the spacecraft positions, to calculate the magnetic field gradient. The current sheet normal ($\boldsymbol{N}$, Figure 2b) is assumed to be along the direction with the maximum magnetic field gradient. The eigenvalue ratio (λ_1/λ_2) between the directions of the maximum and intermediate magnetic field gradient is large (greater than 5, Figure 2d), suggesting that within the tetrahedron of the four spacecraft, the current sheet is mainly a one-dimensional (1D) structure (Shi et al., 2005, 2006). Assuming that the variation of the measured magnetic field over time ($\mathrm{d}\boldsymbol{B}/\mathrm{d}t$) is because the 1D current sheet passes by the spacecraft along $\boldsymbol{N}$, we can obtain the current sheet velocity ($\boldsymbol{V}_{\mathrm{str}} = V_{\mathrm{str}}\boldsymbol{N}$, blue-green-red vector in Figure 2c) by solving the equation $\frac{\mathrm{d}\boldsymbol{B}}{\mathrm{d}t} + V_{\mathrm{str}}(\boldsymbol{N}\cdot\nabla\boldsymbol{B}) = \boldsymbol{0}$ (Shi et al., 2006). As B_x changes from negative to slightly positive, and from positive to negative values again, $\boldsymbol{N}$ mainly lies in the GSM y-z plane with a significant and continuous variation,

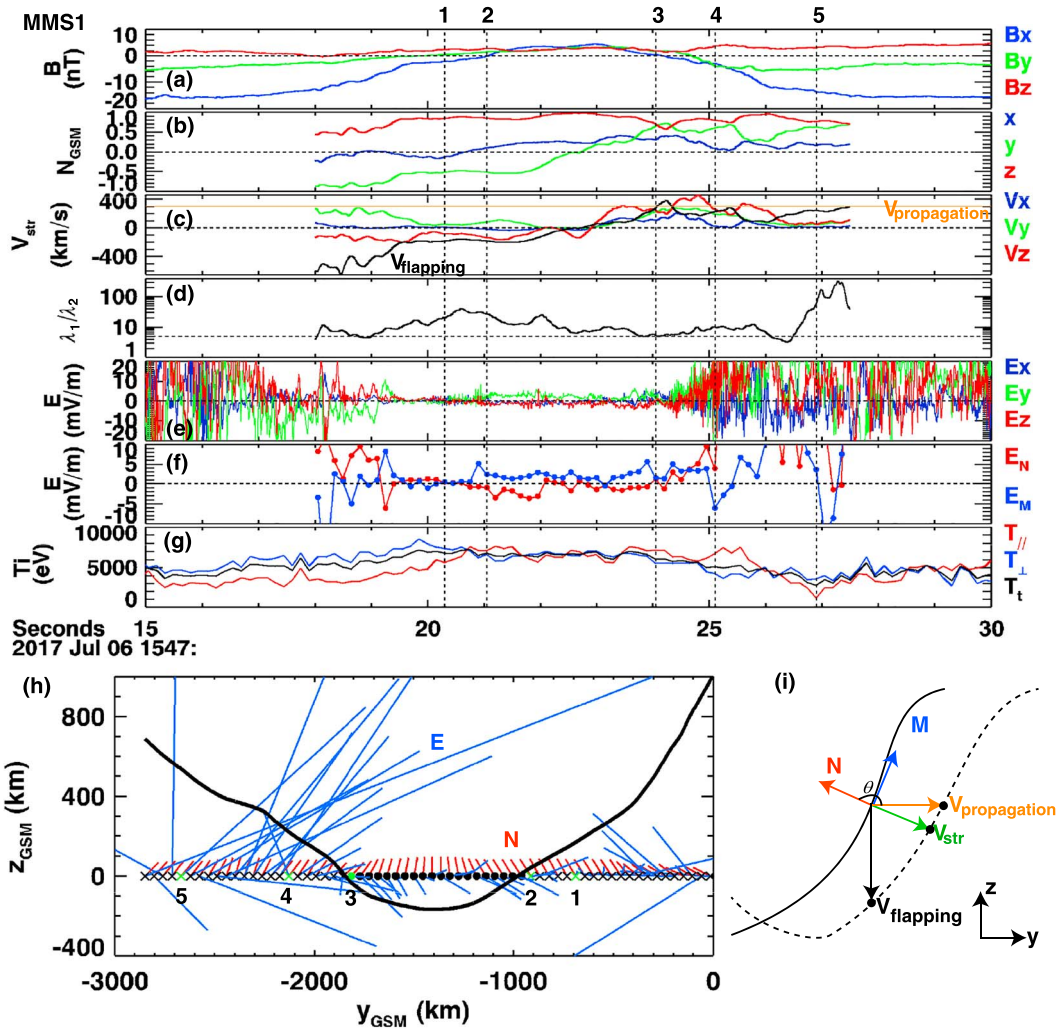

Figure 2. Analysis of the current sheet structure. (a) Magnetic field. (b) The current sheet normal vector in geocentric solar magnetospheric (GSM) obtained from the spatiotemporal difference (STD) method, which continuously changes during the shown interval. (c) The current sheet velocity (V_{str}) along the normal direction (blue, green, and red) obtained from STD. According to the illustration in (i), the orange horizontal line marks the estimated propagation velocity of the current sheet flapping ($V_{propagation}$ = 300 km/s), and the black curve is the estimated flapping velocity ($V_{flapping} = V_{propagation}\cot(\theta)$). (d) The large eigenvalue ratio between the maximum and intermediate magnetic field gradient directions suggests that the current sheet structure within the four spacecraft is mainly one dimensional. (e) Electric fields in GSM. (f) Electric fields normal (E_N) and tangential (E_M) to the current sheet. (g) Ion temperature. (h) The deduced current sheet structure. Each ion distribution location is marked by a cross (if $B_x < 0$) or a dot (if $B_x > 0$). The five locations marked green are for those marked with vertical dashed lines in (a)–(g), and the ion distributions are shown in Figure 3. Red = local normal direction; blue = electric field direction with the length representing $\sqrt{\left(E_y^2 + E_z^2\right)}$.

and the y component of the normal (N_y) reverses the sign. It suggests a kinked current sheet as illustrated in Figure 2h, where the black curve represents the current sheet midplane ($B_x = 0$).

The current sheet structure is further quantitatively determined. The current sheet motion is considered to be a superposition of the up-and-down flapping and the propagation of the flapping. Since the current sheet within the MMS tetrahedron is 1D-like, the STD method only allows us to estimate the motion ($\boldsymbol{V}_{str}$) along the local current sheet normal. We assume that the up-and-down flapping is along z, and the flapping propagates along y. As illustrated in Figure 2i, the flapping propagates from the solid curve to the dashed curve. With the approximation that the three points marked on the dashed curve are aligned on a straight line, the propagation speed is $V_{propagation} = |V_{str}| / |\cos(\theta)|$, where θ is the angle between $\boldsymbol{N}$ and $\boldsymbol{y}$ ($\cos(\theta) = N_y$) and

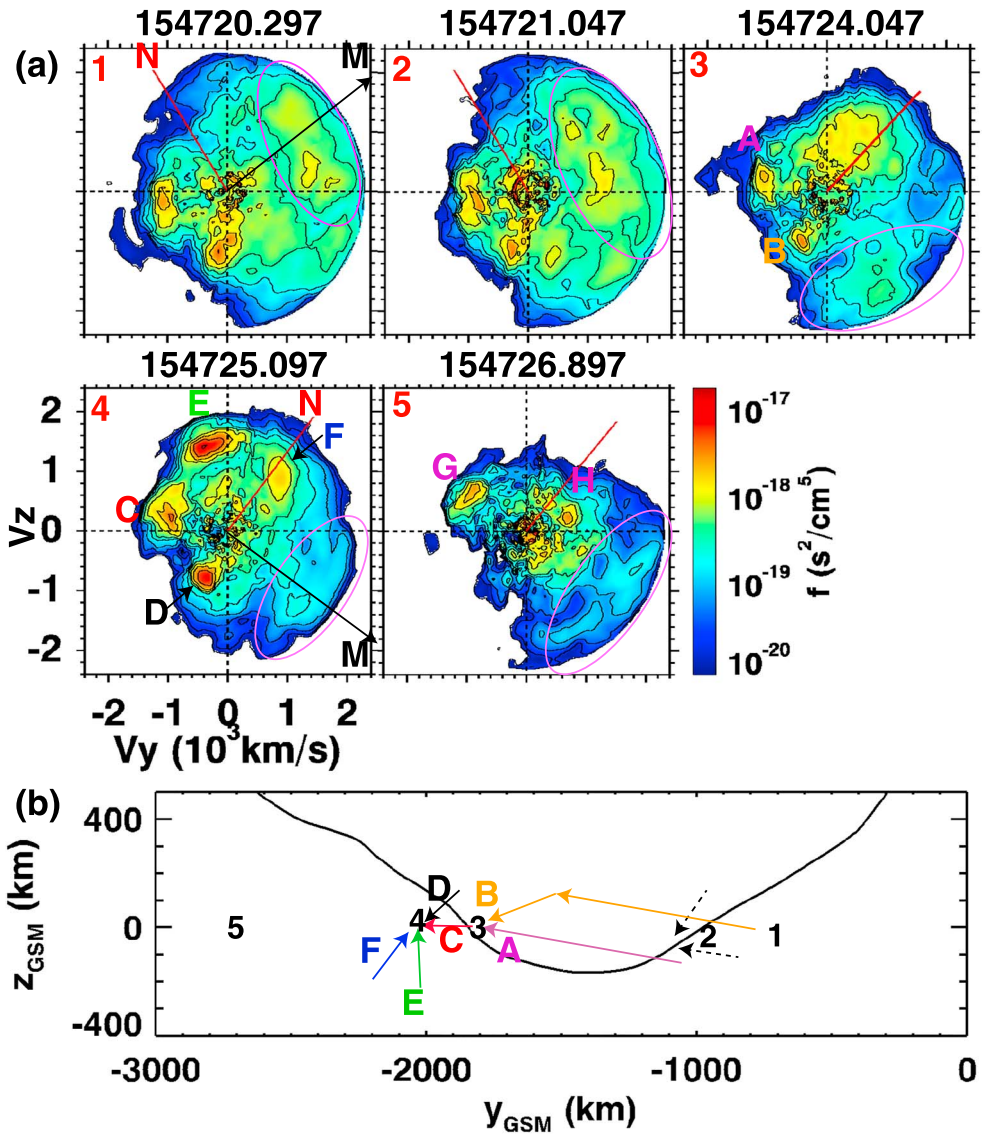

Figure 3. (a) Ion reduced velocity distribution functions in the GSM V_y-V_z plane for locations 1–5. (b) Possible trajectories for populations marked in the distributions. See text for more details.

the direction is toward $y > 0$ since $V_{str,y} > 0$. At locations where $|N_y|$ is large, the propagation speed can be reliably estimated to be $V_{propagation} \sim 300$ km/s (solid horizontal line in Figure 2c), slightly larger than the previous statistical result of tens of kilometers per second to 200 km/s (Sergeev et al., 2004). The flapping velocity is $V_{flapping} = V_{propagation} \cot(\theta)$, with an amplitude of about 500 km/s (black curve in Figure 2c). The current sheet illustration in Figure 2h is determined by integrating the estimated $V_{propagation}$ and $V_{flapping}$, setting $B_x = 0$ close to $z = 0$. For the illustration purpose, the current sheet is plotted as a stationary structure, and the spacecraft moved from $+y$ toward $-y$.

The electric field structure in such a flapping current sheet is close to that in a planar 2D current sheet, yet with modifications. Along $z = 0$, the location of MMS during each ion measurement is marked with a cross (if $B_x < 0$) or a dot (if $B_x > 0$). The five locations in green are for the times marked in Figures 2a–2g, and the corresponding ion distributions are shown in Figure 3. At each location (Figure 2h), the normal direction is marked with a red line, and the electric field direction (averaged during the distribution sampling time) in the y-z plane is marked with a blue line, with the length representing $\sqrt{\left(E_y^2 + E_z^2\right)}$. The

time series of the electric fields in GSM are shown in Figure 2e. The regions with large-amplitude electric fields are close to the separatrix region. Similar to planar current sheets, the electric fields are mainly along $\boldsymbol{N}$ toward the midplane. The clearest deviation between the directions of $\boldsymbol{E}$ and $\boldsymbol{N}$ occurs close to the second midplane crossing (near location 3). Between locations 2 and 3, the electric field directions remain close to the $-\boldsymbol{N}$ direction near the first midplane encounter. The current direction ($\boldsymbol{M}$) is perpendicular to the normal toward $y > 0$. Comparing the angles between $\boldsymbol{E}$ and $\boldsymbol{N}$ vectors, the electric field projection along the current direction (E_M in Figure 2f) is mostly positive, consistent with the reconnection electric field.

Next we discuss the ion distribution features. The five example reduced distributions in the GSM V_y-V_z plane are shown in Figure 3. Distributions from four spacecraft at the same time do not show discernible differences, so only those measured by MMS1 are shown. The red line in each panel marks the local normal direction projected to the y-z plane. In each distribution, an energetic population moves along the current direction (marked by a magenta oval). The local gyroradii of such populations ($|v| \sim 1{,}500$ km/s) are more than 1,000 km, greater than the distance from the current sheet midplane (smaller than 600 km/s). Thus, these ions are doing the meandering motion across the current sheet midplane. Since the reconnection electric field is along the same direction, these ions are likely being accelerated by the reconnection electric field.

At lower energies, multiple ion populations exist. In VDFs 1 and 2, two counterstreaming populations along local $\boldsymbol{N}$ exist, suggesting that the two populations are bouncing in the current sheet and accelerated by E_N. Their M component of the velocity is opposite to the current direction, which is consistent with the direction of the $\boldsymbol{E} \times \boldsymbol{B}$ drift due to the midplane pointing E_N and B_x at large distances from the midplane where ions remain magnetized. The trajectories of counterstreaming populations near location 2 are illustrated in Figure 3b with black dashed arrows. In principle, ions can bounce in the current sheet for multiple times with repeating bouncing trajectories. Between locations 1 and 2, E_N points away from the midplane, which may be a result of a nonzero guide field or the current sheet flapping. Consistently, because location 2 is closer to the current sheet, the separation between the counterstreaming populations is smaller in VDF 2 than in VDF 1.

At location 3, the local $\boldsymbol{N}$ has changed to have a positive y component. However, the alignment of counterstreaming populations (A and B) as well as the electric field direction is close to the normal direction near location 2. One possible explanation is due to the corrugated current sheet structure, and the trajectories of populations A and B are illustrated in Figure 3b with purple and orange arrows, respectively. The counterstreaming ions have negative V_y, such that their entry to the current sheet is at a more positive y location than location 3, where the normal direction may be close to that at location 2. During the bounce motion, these ions arrive at location 3 while exhibiting counterstreaming features along the normal close to their entry location. VDF 3 has an additional population with $V_y > 0$ and $V_z > 0$, which likely has crossed the current sheet midplane from a more negative y location. The population could be either ions that just enter the current sheet from the inflow region for the first time or the counterpart of populations A and B that have bounced back.

VDF 4 contains four discrete populations in addition to the energetic ions along the current direction. The feature can be an effect of the corrugated current sheet, which enables mixing of ions with different velocities. One possible explanation is that populations C and D once were the counterstreaming populations A and B near location 3 that later crossed the current sheet midplane to the $B_x < 0$ side. The trajectories are illustrated with red and black solid arrows, respectively. Populations E and F with opposite normal velocities with those of C and D come from locations further away from the midplane on the $B_x < 0$ side, whose trajectories are illustrated with green and blue arrows, respectively. Populations E and F contain the returning counterparts for populations C and D after one bounce.

VDF 5 no longer has counterstreaming populations along the local $\boldsymbol{N}$. It suggests that the location is close to the edge of the diffusion region and reflection point of bouncing ions, such that populations C and E merge to a single population G, while populations D and F merge to a single population H. The velocity of population G is consistent with the local $\boldsymbol{E} \times \boldsymbol{B}$ drift. Therefore, populations C and E (as well as population A in VDF 3) with the same v_M as in population G can also contain ions that locally enter the current sheet, in addition to ions that travel from the current sheet at more positive y locations.

4. Summary and Discussions

In this study, we have analyzed the current sheet structure and ion behaviors in a magnetotail reconnection diffusion region. The fluctuations of B_x suggest the flapping motion of the current sheet. The analysis of the magnetic fields measured by four spacecraft suggests that the flapping leads to a corrugated shape of the current sheet and the flapping propagates toward the positive GSM y direction with a speed of ~300 km/s.

Ion VDF features suggest that the ion motion is largely controlled by the local current sheet structure (e.g., Nagai et al., 2015; Wygant et al., 2005): Energetic ions move along the local current direction and are likely being accelerated by the reconnection electric field; counterstreaming ions mainly along the local normal direction suggest the acceleration by the Hall normal electric field. The observed electric field indeed shows that the dominant component is along the local normal mainly pointing toward the midplane, and the component tangential to the current sheet is along the current direction.

On the other hand, VDFs at some locations deviate from the expectation for planar current sheets: Counterstreaming ions are not aligned with the local normal (VDF 3 in Figure 3), or more than one pair of counterstreaming populations exist (VDF 4). Here we provide one possible interpretation. Ions have initial velocities along the local normal direction (N_1) upon entering the current sheet. As ions move to a different y location, their velocities appear to be different from the normal direction of the new position (N_2), and they can mix with ions that enter the current sheet at the new position with velocities along N_2. In other words, due to mixing of ions entering at different locations of the corrugated current sheet, the counterstreaming populations do not always align with the local normal direction, and more ion components than predicted in Nagai's study (Nagai et al., 2015) are present—this is the new discovery of the current study with MMS measurements.

We would like to mention that the corrugated current sheet structure and the propagation velocity likely have significant spatial and temporal variations. If the current sheet has a large-scale steady flapping motion, B_x is expected to have fluctuations with similar waveforms for many cycles. However, the waveform of measured B_x fluctuations has much variation over time (Figure 1b), indicating that the estimated current sheet structure in Figure 2h cannot be simply applied to other intervals, and the structure is not repeated for many cycles. It may lead to lack of ion sources at more positive y locations, such that locations 1 and 2 do not have two pairs of counterstreaming populations like at location 4.

We note that the acceleration by the reconnection electric field in a planar current sheet cannot well explain the four populations in VDF 4. It seems to be one explanation if looking at VDF 4 alone. Populations C and E just enter the current sheet with velocities opposite to the current direction. The acceleration by the reconnection electric field during their bouncing motion changes their velocities toward the current direction, which may make them become populations D and F. The acceleration during more bounces would further accelerate ions to be the energetic population marked by the magenta oval. However, it is difficult to explain the difference between VDFs 2 and 4 with such a mechanism.

As shown in Figure 2g, the ion temperature increases from ~4,000 eV near the current sheet boundary with large $|B_x|$ to ~7,000 eV near the current sheet center, which is partially the effective heating due to mixing of different demagnetized ion populations in the diffusion region. The VDFs show that the corrugated current structure enhances the ion mixing (e.g., VDF 4) compared to the VDF structure for planar current sheets (e.g., VDF 2 without much deviation from the planar expectation), though it does not significantly change the effective temperature. The more intense energetic population at positive v_M also leads to a higher temperature at location 2 than at location 4. We expect that the VDFs will be further thermalized in downstream regions, and future studies are needed to see whether the current sheet corrugation and the associated enhanced mixing alter the thermalization process, for example, by affecting the instability conditions.

Acknowledgments
The research is supported in part by a DOE grant DESC0016278, NSF grants AGS-1619584 and AGS-1552142, NASA grants 80NSSC18K1369 and 80NSSC17K0012, and the NASA MMS mission. MMS data are available at MMS Science Data Center (https://lasp.colorado.edu/mms/sdc/).

References

Aunai, N., Belmont, G., & Smets, R. (2011). Proton acceleration in antiparallel collisionless magnetic reconnection: Kinetic mechanisms behind the fluid dynamics. *Journal of Geophysical Research*, *116*, A09232. https://doi.org/10.1029/2011JA016688

Burch, J. L., Moore, T. E., Torbert, R. B., & Giles, B. L. (2015). Magnetospheric multiscale overview and science objectives. *Space Science Reviews*, 1–17. https://doi.org/10.1007/s11214-015-0164-9

Ergun, R. E., Tucker, S., Westfall, J., Goodrich, K. A., Malaspina, D. M., Summers, D., et al. (2016). The axial double probe and fields signal processing for the MMS mission. *Space Science Reviews*, *199*(1-4), 167–188. https://doi.org/10.1007/s11214-014-0115-x

Karimabadi, H., Daughton, W., Pritchett, P. L., & Krauss-Varban, D. (2003). Ion-ion kink instability in the magnetotail: 1. Linear theory. *Journal of Geophysical Research*, *108*(A11), 1400. https://doi.org/10.1029/2003JA010026

Karimabadi, H., Pritchett, P. L., Daughton, W., & Krauss-Varban, D. (2003). Ion-ion kink instability in the magnetotail: 2. Three-dimensional full particle and hybrid simulations and comparison with observations. *Journal of Geophysical Research*, *108*(A11), 1401. https://doi.org/10.1029/2003JA010109

Lindqvist, P.-A., Olsson, G., Torbert, R. B., King, B., Granoff, M., Rau, D., et al. (2016). The spin-plane double probe instrument for MMS. *Space Science Reviews*, *199*(1-4), 137–165. https://doi.org/10.1007/s11214-014-0116-9

Nagai, T., Shinohara, I., & Zenitani, S. (2015). Ion acceleration processes in magnetic reconnection: Geotail observations in the magnetotail. *Journal of Geophysical Research: Space Physics*, *120*, 1766–1783. https://doi.org/10.1002/2014JA020737

Pollock, C., Moore, T., Jacques, A., Burch, J., Gliese, U., Saito, Y., et al. (2016). Fast plasma investigation for magnetospheric multiscale. *Space Science Reviews*, *199*(1-4), 331–406. https://doi.org/10.1007/s11214-016-0245-4

Runov, A., Angelopoulos, V., Sergeev, V. A., Glassmeier, K.-H., Auster, U., McFadden, J., et al. (2009). Global properties of magnetotail current sheet flapping: THEMIS perspectives. *Annales de Geophysique*, *27*, 319–328.

Russell, C. T., Anderson, B. J., Baumjohann, W., Bromund, K. R., Dearborn, D., Fischer, D., et al. (2016). The Magnetospheric Multiscale magnetometers. *Space Science Reviews*, *199*(1-4), 189–256. https://doi.org/10.1007/s11214-014-0057-3

Sergeev, V., Runov, A., Baumjohann, W., Nakamura, R., Zhang, T. L., Balogh, A., et al. (2004). Orientation and propagation of current sheet oscillations. *Geophysical Research Letters*, *31*, L05807. https://doi.org/10.1029/2003GL019346

Sergeev, V., Runov, A., Baumjohann, W., Nakamura, R., Zhang, T. L., Volwerk, M., et al. (2013). Current sheet flappingmotion and structure observed by Cluster. *Geophysical Research Letters*, *30*, 1327. https://doi.org/10.1029/2002GL016500

Sergeev, V. A., Tsyganenko, N. A., & Angelopoulos, V. (2008). Dynamical response of the magnetotail to changes of the solar wind direction: An MHD modeling perspective. *Annales de Geophysique*, *26*, 2395–2402. https://www.ann-geophys.net/26/2395/2008/

Shi, Q. Q., Shen, C., Dunlop, M. W., Pu, Z. Y., Zong, Q. G., Liu, Z. X., et al. (2006). Motion of observed structures calculated from multi-point magnetic field measurements: Application to Cluster. *Geophysical Research Letters*, *33*, L08109. https://doi.org/10.1029/2005GL025073

Shi, Q. Q., Shen, C., Pu, Z. Y., Dunlop, M. W., Zong, Q. G., Zhang, H., et al. (2005). Dimensional analysis of observed structures using multipoint magnetic field measurements: Application to Cluster. *Geophysical Research Letters*, *32*, L12105. https://doi.org/10.1029/2005GL022454

Wygant, J. R., Cattell, C. A., Lysak, R., Song, Y., Dombeck, J., McFadden, J., et al. (2005). Cluster observations of an intense normal componentof the electric field at a thin reconnecting current sheet in the tail and its role in the shock-like acceleration of the ion fluid into the separatrix region. *Journal of Geophysical Research*, *110*, A09206. https://doi.org/10.1029/2004JA010708

Yamada, M., Yoo, J., Jara-Almonte, J., Ji, H., Kulsrud, R. M., & Myers, C. E. (2014). Conversion of magnetic energy in the magnetic reconnection layer of a laboratory plasma. *Nature Communications*, *5*, 4474.

Zenitani, S., Shinohara, I., Nagai, T., & Wada, T. (2013). Kinetic aspects of the ion current layer in a reconnection outflow exhaust. *Physics of Plasmas*, *20*, 092120. https://doi.org/10.1063/1.4821963

Zhang, T. L., Baumjohann, W., Nakamura, R., Balogh, A., & Glassmeier, K.-H. (2002). A wavy twisted neutral sheet observed by Cluster. *Geophysical Research Letters*, *29*(19), 1899. https://doi.org/10.1029/2002GL015544